

# Optical millimeter-wave generation based on period-one oscillation in VCSELs subject to optical injection

ZONG-MIN LENG<sup>a</sup>, GUANG-QIONG XIA<sup>a,b</sup>, ZHENG-MAO WU<sup>a\*</sup>

<sup>a</sup>*School of Physics, Southwest University, Chongqing 400715, China*

<sup>b</sup>*State Key Laboratory of Millimeter Waves, Southeast University, Nanjing 210096, China*

In this paper, based on period-one oscillation in vertical-cavity surface-emitting lasers (VCSELs) subject to optical injection, a novel millimeter-wave generation method is proposed and investigated. The results show that the optical spectrum of optical millimeter-wave consists of only two main components namely single sideband, which is helpful for overcoming the power penalty due to optical fiber dispersion. Through adjusting the injection strength and the frequency detuning between master-VCSEL and slave-VCSEL, optical millimeter-wave with different frequency can be obtained.

(Received June 26, 2009; accepted July 20, 2009)

*Keywords:* Vertical-cavity surface-emitting lasers (VCSELs), Optical injection, Period-one oscillation, Millimeter-wave

## 1. Introduction

Millimeter-wave communication has been a research hot for its great transmission capacity and high transmission frequency in recent years [1]. Generally, via by air, millimeter-wave cannot transmit signals over a long distance due to large attenuation. Therefore, a new technology of radio over fiber (ROF), which integrates millimeter-wave wireless transmission and fiber wired transmission, have attracted considerable interests for such ROF systems are capable of realizing long distance transmission of millimeter-wave signals [2-5]. At present, most of ROF systems are subject to the chromatic dispersion-induced millimeter-wave power penalty. Because the dispersion introduces a phase difference between the sidebands from the optical carrier, the generated beat signals between the sidebands and the carrier may add up destructively depending on their phase relationship. As a result, the generated millimeter-wave power will suffer an obvious reduction.

Power penalty can be avoided by using the single sideband (SSB) modulation scheme, where the radio frequency (RF) output signal is generated by only two optical bands, namely the optical carrier and the first sideband [6-10]. Different SSB optical microwave or millimeter-wave sources have been reported such as two

lasers heterodyning [11-12], SSB external modulators [13], dual-mode or multisection semiconductor lasers [3, 14] and harmonic upconversion in nonlinear lasers [15]. In this paper, a novel method to generate millimeter-wave based on period-one oscillation in a slave vertical-cavity surface-emitting laser (S-VCSEL) subject to optical injection from a master VCSEL (M-VCSEL) is proposed. This system employs a self-heterodyne arrangement in which a dual-frequency optical source generates a low phase-noise millimeter-wave beat signal via by a high-speed photodiode. Through adjusting the injected strength and the frequency detuning between the S- and M-VCSEL, optical millimeter-wave with different frequency can be obtained.

## 2. Model

The systematical configuration is schematically shown in Fig. 1. The output of the M-VCSEL is unidirectionally coupled into the S-VCSEL by an optical isolator (OI), and a variable attenuator (VA) is used to adjust the injected strength. The output of the S-VCSEL is divided into  $x$  and  $y$  linear polarization (LP) modes by a polarizing beam splitter (PBS), and the optical spectrum and the power spectrum are monitored by a optical spectrum analyzer

(OSA) and a power spectrum analyzer (PSA), respectively.

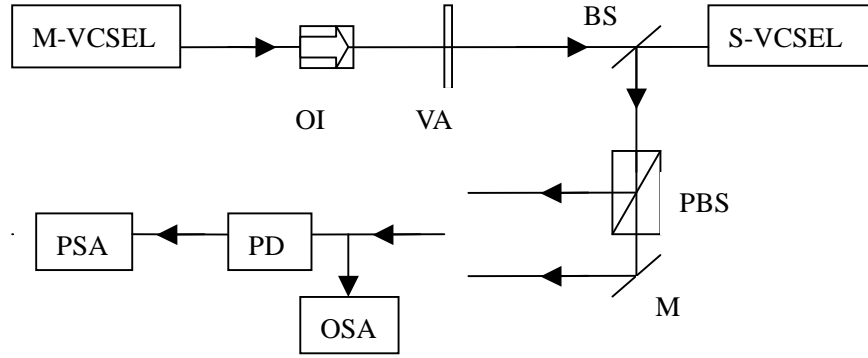


Fig. 1. Schematic diagram of the proposed setup. M-VCSEL: master VCSEL; S-VCSEL: slave VCSEL; OI: optical isolator; VA: variable attenuator; BS: beam splitter; PBS: polarizing beam splitter; M: mirror; PD: photodiode; PSA: power spectrum analyzer; OSA: optical spectrum analyzer.

Based on the spin-flip model (SFM) [16], the rate equations for the M-VCSEL and S-VCSEL with optical injection can be described by:

$$\dot{E}_x^m = \kappa(1+i\alpha)(N^m E_x^m + in^m E_y^m - E_x^m) - (i\gamma_p + \gamma_a)E_x^m + F_x^m \quad (1)$$

$$\dot{E}_y^m = \kappa(1+i\alpha)(N^m E_y^m - in^m E_x^m - E_y^m) + (i\gamma_p + \gamma_a)E_y^m + F_y^m \quad (2)$$

$$\dot{E}_x^s = \kappa(1+i\alpha)(N^s E_x^s + in^s E_y^s - E_x^s) - (i\gamma_p + \gamma_a)E_x^s + \eta E_x^m(t-\tau)\exp[-i2\pi(\nu^m\tau - \Delta\nu t)] + F_x^s \quad (3)$$

$$\dot{E}_y^s = \kappa(1+i\alpha)(N^s E_y^s - in^s E_x^s - E_y^s) + (i\gamma_p + \gamma_a)E_y^s + \eta E_y^m(t-\tau)\exp[-i2\pi(\nu^m\tau - \Delta\nu t)] + F_y^s \quad (4)$$

$$\dot{N}^{m,s} = -\gamma[N^{m,s}(1 + |E_x^{m,s}|^2 + |E_y^{m,s}|^2) - \mu + in^{m,s}(E_y^{m,s} E_x^{m,s*} - E_x^{m,s} E_y^{m,s*})] \quad (5)$$

$$\dot{N}^{y,s} = -\gamma_s n^{m,s} - \gamma[n^{m,s}(|E_x^{m,s}|^2 + |E_y^{m,s}|^2) + iN^{m,s}(E_y^{m,s} E_x^{m,s*} - E_x^{m,s} E_y^{m,s*})] \quad (6)$$

where superscripts  $m$  and  $s$  represent the M-VCSEL and S-VCSEL, respectively, and subscripts  $x$  and  $y$  represent  $x$ - and  $y$ - LP modes, respectively.  $E$  is the slowly varying

amplitude,  $N$  is the total carrier inversion between conduction and valence bands,  $n$  is the difference between carrier inversions with opposite spins,  $\kappa$  is the photon decay rate,  $\alpha$  is the linewidth enhancement factor,  $\gamma$  is the carrier decay rate,  $\gamma_s$  characterizes microscopic processes leading to the homogenization of carrier spin,  $\gamma_a$  and  $\gamma_p$  depict the linear cavity dichroism and phase anisotropy, respectively,  $\mu$  is the normalized injection current,  $\nu$  is the laser frequency and  $\Delta\nu = \nu^m - \nu^s$  is the frequency detuning,  $\tau$  is the coupling retardation time from M-VCSEL to S-VCSEL,  $\eta$  is the injection strength, and the spontaneous emission noises are described by following Langevin sources:

$$F_x^{m,s} = \sqrt{\beta_{sp}/2}(\sqrt{N^{m,s} + n^{m,s}}\xi_1^{m,s} + \sqrt{N^{m,s} - n^{m,s}}\xi_2^{m,s})$$

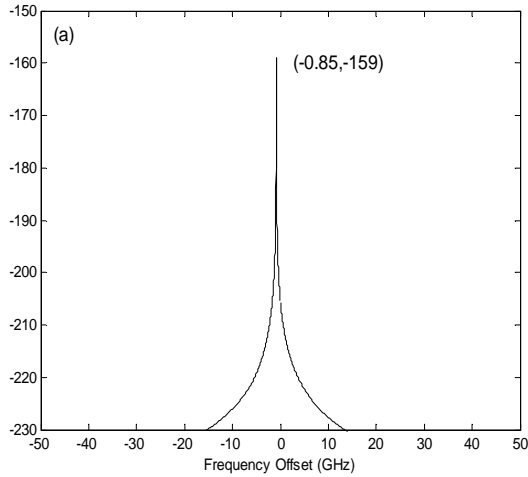
$$F_y^{m,s} = -i\sqrt{\beta_{sp}/2}(\sqrt{N^{m,s} + n^{m,s}}\xi_1^{m,s} - \sqrt{N^{m,s} - n^{m,s}}\xi_2^{m,s})$$

where  $\xi_1$  and  $\xi_2$  are independent Gaussian white noise with zero mean and unitary variance, and  $\beta_{sp}$  is spontaneous emission rate [17].

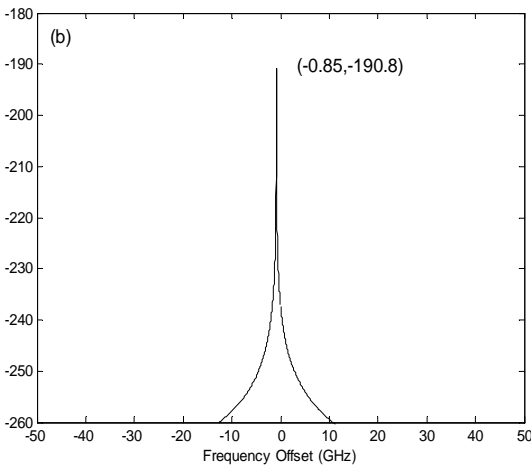
### 3 Results and discussion

The rate equations mentioned above can be numerically solved by the fourth-order Runge-Kutta method. During the calculations, the used parameters are

[16, 17]:  $\kappa=300ns^{-1}$ ,  $\alpha=3.5$ ,  $\gamma=1ns^{-1}$ ,  $\gamma_s=50ns^{-1}$ ,  $\gamma_p=6ns^{-1}$ ,  $\gamma_a=0.1ns^{-1}$ ,  $\tau=3ns$ ,  $\mu=1.3$ ,  $\beta_{sp}=10^{-6}ns^{-1}$ ,  $\nu=193.5THz$  (corresponding wavelength is 1550 nm).



(a)



(b)

Fig. 2. Optical spectrum of the M-VCSEL, where (a) and (b) depict *x*- and *y*-LP modes, respectively.

Fig. 2 gives the optical spectrum of the M-VCSEL for. From this diagram, it can be seen that both the central wavelengths of *x*-LP and *y*-LP mode are not located at 1550nm and the shifting value is about -0.85GHz for both *x*-LP mode and *y*-LP mode for  $\gamma_p=6 ns^{-1}$ . Under this condition, the frequency detuning  $\Delta\nu=30GHz$  means exact frequency detuning for *x*-LP mode and *y*-LP mode between M-VCSEL and S-VCSEL is 29.15GHz. For above given parameters, the output power of *x*-LP mode is much larger than that of *y*-LP mode.

The optical spectra of S-VCSEL under optical injection of M-VCSEL are shown in Fig. 3 for  $\Delta\nu=30GHz$  and different injected strengths, where the left and right columns correspond to *x*-LP mode and *y*-LP mode, respectively. It should be pointed out that the frequency axis is offset to the free-running frequency of the S-VCSEL. As shown in fig. 3 (a), for  $\eta=198ns^{-1}$ , the injection power is large enough to lock the S-VCSEL to the frequency of M-VCSEL. When  $\eta$  decreases to  $160ns^{-1}$  (see fig. 3(b)), the S-VCSEL enters the period-one state under this proper injection strength, and the corresponding optical spectrum of S-VCSEL consists of two main components. One component is the injection frequency  $f_i$ , the other is the carrier frequency  $f_c=f_i-f_m$ , and their frequency difference is equivalent to the millimeter-wave frequency  $f_m=30.73 GHz$ . For  $\eta=70 ns^{-1}$  as shown in Fig. 3 (c), the according millimeter-wave frequency is 30.14 GHz. Furthermore, there appears second sideband at an even lower optical frequency, and its height is so small compared to the two main components that can be neglected,

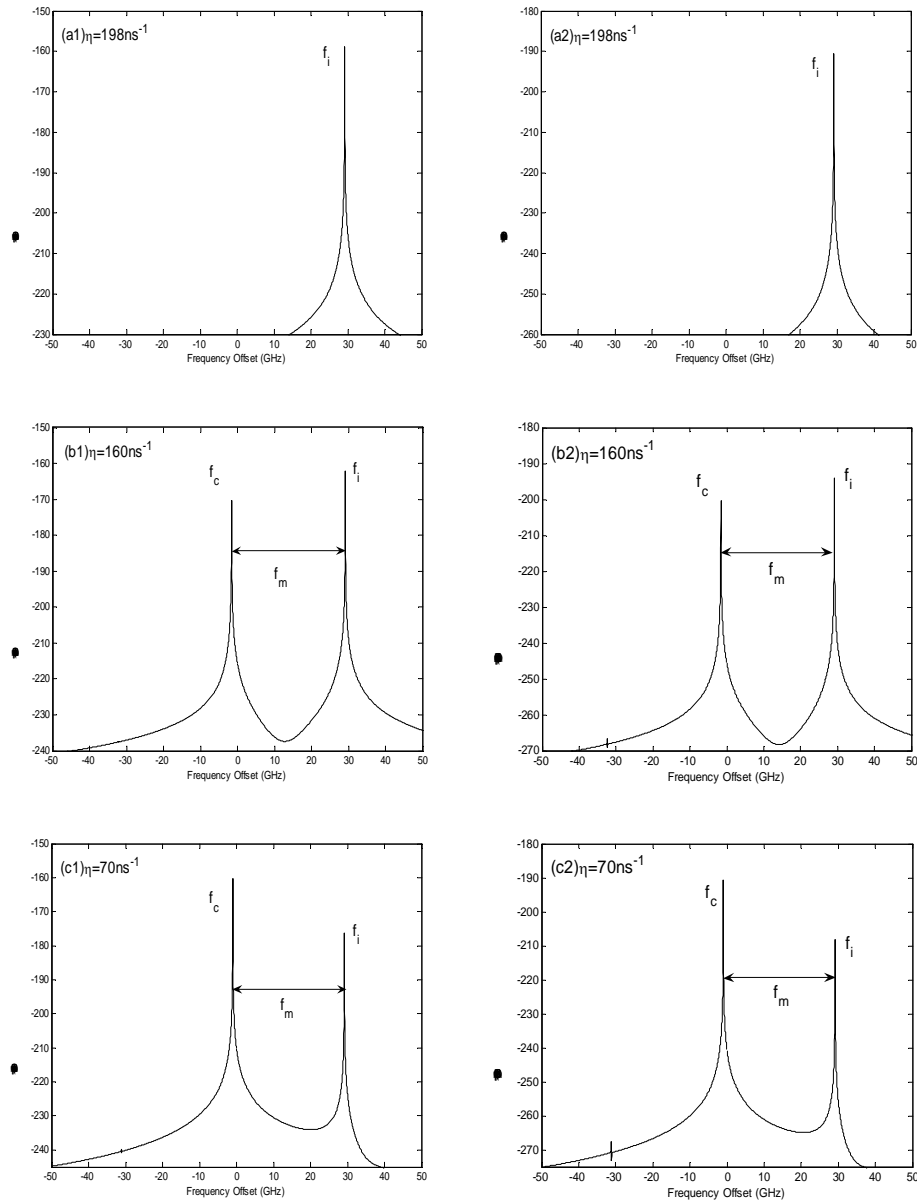


Fig. 3. Optical spectra of the S-VCSEL for  $\Delta\nu=30\text{GHz}$  and different injected strength, where the left and right columns correspond to x-LP mode and y-LP mode, respectively.

Usually, the dynamics of a VCSEL under optical injection is different from that of an edge-emitting semiconductor laser under optical injection [18]. As mentioned in Ref. [18], period-one oscillation in a edge-emitting semiconductor laser can behave SSB or DSB depending on the injection strength  $\eta$ .

However, for an optical injection VCSEL operates at period-one state, calculations show that both x-LP mode and y-LP mode only exhibit SSB period-one oscillation. Therefore, an optical injection VCSEL may be one of excellent sources for the millimeter-wave generation in a ROF system.

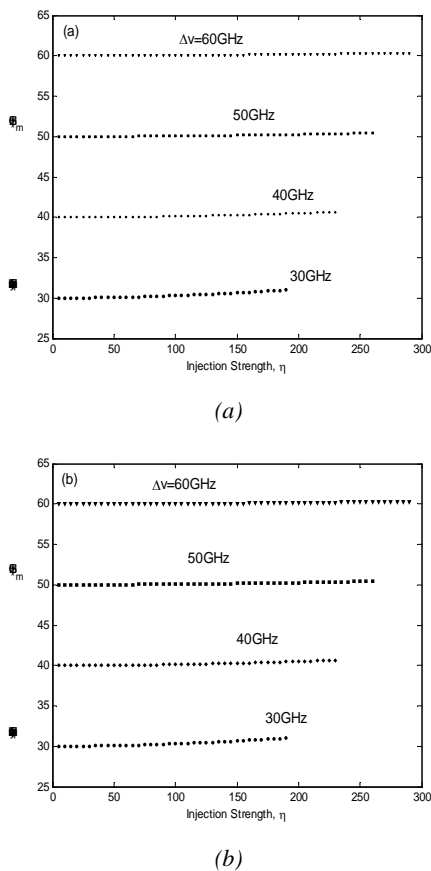


Fig. 4. Millimeter-wave frequency  $f_m$  as a function of the injection strength for different frequency detuning, where (a) and (b) depict  $x$ - and  $y$ -LP modes, respectively.

Fig. 4 shows millimeter-wave frequency  $f_m$  as a function of the injection strength  $\eta$  for different frequency detuning. For a fixed frequency detuning, the millimeter-wave frequency increases with the increase of the injection strength. It can be due to the red-shifting of the cavity resonance. When injection strength increases, the optical gain deficit increases [19-20]. Because of the antiguidance effect, the refractive index increases and the cavity resonance shifts red. The red-shifting causes the carrier frequency  $f_c$  decrease. Hence, if one needs a larger millimeter-wave frequency  $f_m$ , a larger injection power will be necessary. Additionally, with the increase of the frequency detuning, the antiguidance effect will be weakened, so the influence of the injection strength on the millimeter-wave frequency will be decreased. When the frequency detuning increases to 60 GHz, the millimeter-wave frequency is near to be a constant and do not vary with the increase of the injection strength.

#### 4. Conclusions

In summary, a novel approach to generate millimeter-wave based on period-one oscillation in optical injection VCSELs has been presented and investigated. The system employs a self-heterodyne arrangement in

which a dual-frequency optical source generates a millimeter-wave beat signal via by a high-speed photodiode. Under proper injection strength, the S-VCSEL only oscillates at a SSB period-one state. This is different from that case in a edge-emitting semiconductor laser under optical injection where period-one oscillation can behave SSB or DSB. Through adjusting the injection strength and the frequency detuning between M-VCSEL and S-VCSEL, wide frequency tuning range of millimeter-wave can be obtained. This work shows that the optical injected VCSEL operated at the period-one state can be served as an attractive source for delivering millimeter-wave signals over fibers.

#### Acknowledgements

This work was supported by the Open Fund of the State Key Laboratory of Millimeter Waves of China under Grant K200805, and the Natural Science Foundation Project of Chongqing City of China under Grant 2007BB2333.

#### References

- [1] J. Y. Park, S. S. Jeon, Y. X. Wang, T. Itoh, IEEE Trans. Microw. Theory Tech. **51**, 1482 (2003).
- [2] K. Kitayama, A. Stohr, T. Kuri, R. Heinzelmann, D. Jager, Y. Takahashi, IEEE Trans. Microw. Theory Tech. **48**, 2588 (2000).
- [3] C. Lim, D. Novak, A. Nirmalathas, G. H. Smith, IEEE Trans. Microw. Theory Tech. **49**, 288 (2001).
- [4] S. T. Choi, K. S. Yang, S. Nishi, S. Shimizu, K. Tokuda, Y. H. Kim, IEEE Trans. Microw. Theory Tech. **54**, 1953 (2006).
- [5] D. Novak, G. H. Smith, A. J. Lowery, H. F. Liu, R. B. Waterhouse, Opt. Quantum Electron. **30**, 1021 (1998).
- [6] S. C. Chan, J. M. Liu, IEEE J. Quantum Electron. **42**, 699 (2006).
- [7] Y. C. Shen, X. M. Zhang, K. S. Chen, IEEE Photon. Technol. Lett. **17**, 1277 (2005).
- [8] S. R. Blais, J. Yao, IEEE Photon. Technol. Lett. **18**, 2230 (2006).
- [9] G. H. Smith, D. Novak, Z. Ahmed, Electron. Lett. **33**, 74 (1997).
- [10] F. Ramos, J. Marti, IEEE Photon. Technol. Lett. **11**, 1479 (1999).
- [11] J. T. Kim, Int. J. Electron. Commun. **60**, 71 (2006).
- [12] G. J. Simonis, K. G. Purchase, IEEE Trans. Microw. Theory Tech. **38**, 667 (1990).
- [13] G. H. Smith, D. Novak, Z. Ahmed, IEEE Trans. Microw. Theory Tech. **45**, 1410 (1997).
- [14] D. Wake, C. R. Lima, P. A. Davies, IEEE Trans. Microw. Theory Tech. **43**, 2270 (1995).
- [15] R. P. Braun, G. Grosskopf, R. Meschenmoser, D. Rohde, F. Schmidt, G. Villino, Electron. Lett. **33**, 1884 (1997).

- [16] J. M. Regalado, F. Prati, M. San Miguel, N. B. Abraham, *IEEE J. Quantum Electron.* **33**, 765 (1997).
- [17] I. Gatara, M. Sciamanna, A. Locquet, K. Panajotov, *Opt. Lett.* **32**, 1629 (2007).
- [18] S. C. Chan, S. K. Hwang, J. M. Liu, *Opt. Express*, **15**, 14921 (2007).
- [19] T. B. Simpson, J. M. Liu, A. Gavrielides, *IEEE J. Quantum Electron.* **32**, 1456 (1996).
- [20] A. Murakami, K. Kawashima, K. Atsuki, *IEEE J. Quantum Electron.* **39**, 1196 (2003).

---

\*Corresponding author: zmwu@swu.edu.cn